

# Global geothermal electricity potentials: A technical, economic, and thermal renewability assessment

D. Franzmann<sup>a,b,\*</sup>, H. Heinrichs<sup>a</sup>, D. Stolten<sup>a</sup>

<sup>a</sup> Forschungszentrum Jülich GmbH, Institute of Energy and Climate Research – Jülich Systems Analysis (ICE-2), 52425 Jülich, Germany

<sup>b</sup> RWTH Aachen University, Chair for Fuel Cells, Faculty of Mechanical Engineering, 52062, Aachen, Germany

## ARTICLE INFO

Dataset link: [Global Technical Energy Potentials of Enhanced Geothermal Systems \(Original data\)](#)

### Keywords:

EGS  
Global energy potential  
Dispatchable renewable energy  
Land eligibility analysis  
Potential analysis  
Hot dry rock

## ABSTRACT

Geothermal energy can play an important role in dispatchable power generation. However, no detailed global energy potential exists. This study calculates the global energy potential for enhanced geothermal power and determines its impact on the energy supply of countries. In this work, the first detailed land eligibility analysis for enhanced geothermal power is conducted, three reservoir models (Gringarten, Volume Method and Sustainable Approach) are compared. The results show that land eligibility is highly dependent on local conditions and varies from <5 to 72 % eligibility with a global average of 25 %. The Gringarten model is the only one to reach realistic production rates and thus economically feasible production plants. Global hotspots for geothermal power below 5 ct<sub>e</sub>/kWh<sub>el</sub> are found in 17 specific countries in the developing world, as well as in Russia, Iceland, Hungary and Japan. Below 10 ct<sub>e</sub>/kWh<sub>el</sub>, potential can be found throughout the Americas, Africa and Southeast Asia. Therefore, deep geothermal energy can be a cheap and reliable source of electricity for developing countries. However, its use for developing countries depends on the cost reduction for geothermal drilling by the developed nations. For countries such as USA, Japan, China, geothermal power can only partially supply their energy systems.

## 1. Introduction

The urgent need to mitigate climate change and reduce greenhouse gas emissions has accelerated the global transition to renewable energy sources. Among these, geothermal energy stands out as an attractive option due to its ability to provide a continuous and dispatchable supply of electricity, independent of weather conditions. Van der Zwaan et al. [1] project, that about 800–1300 TWh/yr of geothermal energy could be used in 2050.

For power generation, only deep geothermal heat generation below about 400 m depth can be used, as thermal conversion requires minimum temperatures of 150 °C [2]. This can only be achieved by hydrothermal or petrothermal heat extraction (also called enhanced geothermal systems, EGS, or hot dry rock, HDR). Enhanced geothermal systems do not rely on the presence of aquifers as hydrothermal systems and can therefore provide an abundance of technical potential at different locations around the globe [2]. Stober et al. [3] estimate the future cost of EGS electricity to be less than 5 ct\$/kWh<sub>el</sub> in the US. This cost projection is consistent with the efforts of the US Office of Energy Efficiency & Renewable Energy, which is targeting for 5 ct\$/kWh<sub>el</sub> from

EGS in 2035 [4]. Based on 64 existing EGS installations [5], this technology can be classified as a technology readiness level 7 or higher [6]. Therefore, enhanced geothermal systems can play an important role in providing low-cost dispatchable power in the future.

Several studies have calculated the technical energy or capacity potential of geothermal energy for different regions. Most of these studies use the volume method introduced by Tester et al. [2] and further developed by Beardsmore et al. [7], which estimates the electrical power output of an EGS plant based on the thermal enthalpy of the reservoir volume for an assumed thermal drawdown, an assumed recovery factor, and the thermal conversion efficiency based on the host rock temperature. This method has been applied by Jung et al. [8] for Germany, Tester et al. [2] and Augustine et al. [9] for the US, Chamorro et al. [10] and Limberger et al. [11] for Europe and Aghahosseini et al. [12] for the world. However, the uncertainties in the academic literature are high. For Europe, the results of Limberger et al. [11] and Chamorro et al. [10] differ by a factor of 4. For the United States, results of Aghahosseini et al. [12] and Tester et al. [2] differ by a factor of 4.7. The major difference are the different assumptions for land eligibility and assumptions for the operation, such as thermal drawdown and recovery

\* Corresponding author. Forschungszentrum Jülich GmbH, Institute of Energy and Climate Research – Jülich Systems Analysis (ICE-2), 52425, Jülich, Germany.  
E-mail address: [d.franzmann@fz-juelich.de](mailto:d.franzmann@fz-juelich.de) (D. Franzmann).

factor. Also, no study provides a detailed spatial analysis of the land eligibility as done for other renewable energies as in Ryberg et al. [13]. In addition, only Aghahosseini et al. [12] and Chamorro et al. [10] evaluate the impact of a different operation strategy by exploring the energy potential for sustainable heat and power. However, the approach of Gringarten et al. [14], further investigated by Doe et al. [15], has never been used in a technical potential analysis. Finally, all the above models, if using a cost model, calculate the LCOE independently of the model for the technical potential, thus missing the linkage of the production rate from the technical analysis to their economic models.

This study tries to fill these research gaps by answering the following research questions: 1) How large is the EGS energy potential considering detailed land eligibility analysis? 2) What is the best way to operate EGS plants? 3) What are the global potentials in terms of energy and cost and where can a country's energy system best benefit from EGS plants? Therefore, a detailed land eligibility for EGS is applied which is the first of its kind in the literature. Then, different reservoir simulation models from the literature are evaluated and compared with actual plant data to understand the differences in these approaches. Finally, the technical energy potential is presented and the impact of EGS on the energy supply of countries is drawn.

## 2. Methodology

A five-step approach is developed to calculate the global technical energy potential and levelized cost of electricity (see Fig. 1). First, a global land eligibility analysis is performed to determine location specific placements of potential EGS plants globally. Next, geological temperatures are derived globally for the suitable depth range of 0–7000 km. Reservoir models found in the literature are then applied to the placements and geological temperatures to determine the technical power output of enhanced geothermal power production. Finally, economic and renewability parameters are defined to evaluate the different simulation models from technical, economic and renewability aspects.

### 2.1. Land eligibility for EGS

The land eligibility analysis for geothermal power plants identifies all eligible areas for EGS plants worldwide. Among the different EGS potential approaches previously discussed, the most promising framework is developed by Ryberg et al. [13], who developed a location-specific evaluation of PV and onshore wind placements for Europe within his developed framework GLAES (Geospatial Land Availability for Energy Systems) [16]. GLAES is a tool for evaluating the eligible land for placing renewable energy sources based on different open source datasets on a 100m grid globally. Consequently, GLAES is used in this analysis to perform the land eligibility analysis globally. A 100m × 100m grid evaluation is chosen as a trade-off between accuracy and computational feasibility. Therefore, 25 different land use categories are iteratively excluded until only the eligible area remains. The most relevant land usage restrictions are a minimal distance of 300 m to settlements due to noise [17], the exclusion of nature protected areas, regions with high water scarcity due to the water demand of the plants [2] and a slope of higher than 17° (see Table 1). The detailed datasets are presented in the Appendix. The land use criteria of Garrison et al. [17] are applied, as they performed the most detailed site-specific analysis of the suitability of enhanced geothermal plants found in literature. Due to the acoustic noise of the plant itself of about 83 dB [17], a minimum

**Table 1**

Exclusion criteria of enhanced geothermal plants.

Nr	Buffer	Applied to land use category	Reason for exclusion
1	300 m	Settlements, industrial areas	Acoustic impact [17]
2	300 m	nature protected areas, intact forest,	Nature protection [17]
3	100 m	Roads, train lines, power lines, etc.	Geometric distance to infrastructure [13]
4	100 m	Slopes >17°	Maximum slope of the plant [18]
5	0 m	Rivers, creeks, seas	Land use
6	0 m	Water scarcity	Water scarcity
7	900 m	Dunes	Movement of dunes

distance of 300 m to all global settlements as well as protected areas is required. Also, all infrastructure is excluded with a distance of 100 m as well as slopes are limited due to a maximum slope of building the plant at 17° [18]. All water areas are also excluded. Agricultural areas such as pastures, croplands, and forests are not excluded because deep geothermal plants typically do not have high land use. These can be as low as 1.1 % according to the Soultz EGS plant [2], resulting in a minimal impact on land use. To preserve intact forests [19] such as the rainforest, those are also excluded for conservation reasons. Due to the loss of up to 5 % of production water [2], which has to be replaced during operation, regions with a high water scarcity definition based on Hofste et al. [20], are not considered for the operation of deep geothermal plants. The detailed underlying data sets for the land eligibility analysis are presented in Table 3.

### 2.2. Placement of location specific plants

After determining the suitable land areas globally, location-specific placements are derived for the subsequent geological simulation. A simple plant design is used: Each individual plant is operated in a doublet configuration with one injection and one production well per plant. For existing plants and previously discussed EGS simulation approaches, the average reservoir size for each plant is about 1 km<sup>3</sup> with an average borehole spacing of 1 km. Additionally, when different enhanced geothermal plants are placed next to each other, the interchange between these plants must be prevented. This is mainly due to the unpredictability of the reservoir stimulation, which results in a non-uniform fracture network around the wells [21]. If the plants are located too close to each other, there is a chance that the reservoirs of neighboring plants will be interconnected, which in the worst case can lead to a thermal short circuit that renders both reservoirs unusable [22]. Therefore, additional spacing is assumed to prevent such interactions of the reservoirs. Since enhanced geothermal systems are not yet deployed to an extent, the interaction of neighboring reservoirs is of concern, there is little research or practical evidence in this area. The only study found that considers the exchange of reservoirs is by Willems et al. [23], who investigated the interchanges of reservoirs for hydrothermal plants. According to this study, an additional buffer distance of 50 % of the borehole spacing is required to prevent interchanges, resulting in the plant spacing as shown in Fig. 2. Finally, based on the determined eligible land raster, the spacing of the plants and the methodological approach for deriving location specific placements described in Ryberg et al. [13], a theoretical set of global location specific plants is derived.

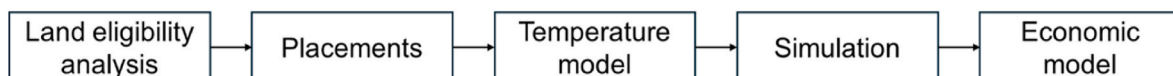


**Fig. 1.** Applied approach for determining the global geothermal energy cost-potential.

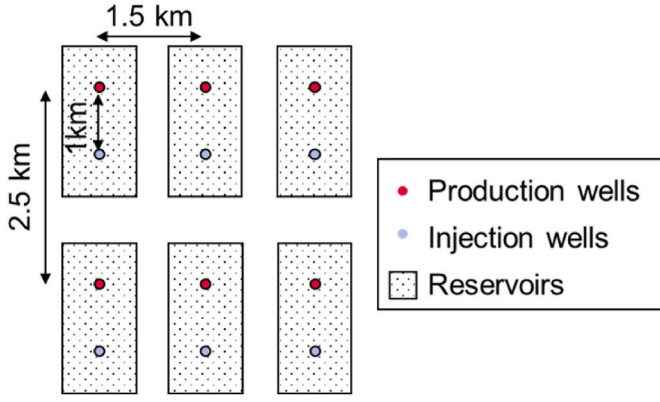


Fig. 2. Spacing of deep geothermal reservoirs and their boreholes for the global location specific distribution of plants.

### 2.3. Geological resources

Once the plant locations have been identified, the underlying geological resources must be determined. In order to utilize enhanced geothermal systems, two criteria must be met: There must be a fractured host rock and a temperature high enough to operate a thermal power plant [2]. The first condition is usually met, as the crystalline basement and therefore host rock can be found at technically drillable depths [24]. However, the second criterion is more relevant because the temperature has a strong influence on the amount of energy available and the thermodynamic efficiency of power generation. To model the heat extraction from the reservoir, the geological temperatures are required for all technically drillable depths up to 7000 m [8]. Measured data are compiled in the “Global data base for borehole temperatures” [25], but lack the uniform geospatial resolution needed for this work. Artemieva et al. [26] publish uniform geological temperatures at the depth of the Earth’s crust at a discretization of 50 km, making the data unusable for the analysis of this paper due to the broad resolution. To tackle this, studies for geothermal analysis as Aghahosseini et al. [27] and Limberger et al. [11] model geological temperatures for different parts of the world based on heat flow equations. Both approaches assume a steady state heat flow without heat advection and do not account for local anomalies below a  $1^\circ \times 1^\circ$  resolution. This work also uses these established approaches [11,12] by solving the heat flow equations in the Earth’s crust [3] for the temperature  $T$  at depth  $z$ :

$$T(z) = T_{surf} + \frac{\dot{q}_{surf}}{\lambda_{Earth}} z - \frac{A}{2 \lambda_{Earth}} z^2 \quad (1)$$

Where  $T_{surf}$  is the mean surface temperature,  $\dot{q}_{surf}$  is the surface heat flux,  $A$  is the radiogenic heat generation and  $\lambda_{Earth}$  is the heat transfer coefficient of the rock. The equation is calculated based on the model of Hartmann and Moosdorf [28], which describes the rock properties globally on a  $0.5^\circ \times 0.5^\circ$  grid. Based on the lithology, the average heat transfer  $\lambda_{Earth}$  is determined using the assumptions of Aghahosseini et al. [27], which provide average heat transfer coefficients for a given rock type. The radiogenic heat generation  $A$  is derived from Goutorbe et al. [29]. The mean surface temperature  $T_{surf}$  is used from the NASA POWER data viewer which provides a reasonable resolution [30]. The surface heat flux  $\dot{q}_{surf}$  is based on the geological analysis of Goutorbe et al. [29] on a  $1^\circ \times 1^\circ$  grid globally, which provide the most complete global data due to its similarity approach.

### 2.4. Reservoir modeling

Based on the global set of candidate plants and geological resources, the heat production of the plants can be determined. There are three different approaches in the literature: The Volume Method, the Gringarten Method and the Sustainable Approach. All these methods use different underlying approaches for the operation strategy: The volume method uses a fixed temperature drop of the reservoir and calculates the heat flow based on recovery factors [7]. The sustainable volume method harvests only the full renewable heat from the reservoir [10]. For the Gringarten approach, Gringarten et al. [14] provides analytical solutions for the physical behavior of reservoirs in general, which are combined with an operational strategy in this work. To compare these approaches, they are all applied independently and their results are compared afterwards in order to select the most suited approach.

#### 2.4.1. Volume method

The volume method used in this work is based on the developments of Tester [2] and Beardsmore et al. [7]. The main idea is to calculate the available heat in a reservoir and estimate the recoverable heat  $H_{res,use}$  based on an assumed recovery factor  $R_F$  [2,7]:

$$H_{res,use} = \rho_{rock} c_{p,rock} V_{res} R_F \Delta T \quad (2)$$

The temperature drop of the reservoir volume  $V_{res}$  is assumed to be  $\Delta T = 10K$ , in accordance with common approaches in the literature [11, 12]. The recovery factor is assumed to be  $R_F = 0.14$  based on Beardsmore et al. [7] in agreement with other literature sources such as Aghahosseini et al. [12]. The density of the host rock  $\rho_{Rock}$  is assumed to be  $2.55 \text{ kg/m}^3$  and the heat capacity is assumed to be  $c_{p,Rock} = 1 \text{ kJ/kgK}$  [31,32]. The average production heat flow over the plant lifetime of 30 years [2] can be calculated using the equation from Beardsmore et al. [7]:

$$\dot{Q}_{pr} = \frac{H_{res,use}}{n_{lifetime}} \quad (3)$$

Heat is supplied at the average production water temperature  $T_{pr}$  based on the host temperature  $T_{Rock}$  at depth of the reservoir [2].

$$T_{pr} = T_{rock} - \frac{\Delta T}{2} \quad (4)$$

#### 2.4.2. Sustainable volume method

The reservoir temperature drop  $\Delta T$  is set to zero for the renewable operation of the plants, that do not use depleting heat sources of the reservoir. The sustainable volume method is based on and named by literature approaches [10,12]. Instead, the production well heat flow is based on the geological heat flow:

$$\dot{Q}_{pr} = \dot{q}_{surf} x_{res} y_{res} \quad (5)$$

where  $x_{res} y_{res}$  is the horizontal area of the reservoir of  $1 \text{ km}^2$ . The heat is available at the temperature level of the natural reservoir  $T_{pr} = T_{Rock}$ , since there is no temperature drop when using the sustainable method.

#### 2.4.3. Gringarten approach

In order to describe the reservoir behavior without detailed simulations, Gringarten et al. [14] calculated the analytical solutions for the outlet temperature of the reservoir of EGS power plants. These equations have already been applied by Doe et al. [15] to calculate the mass flow of production water for a technical potential analysis of EGS heat production. In contrast, in this work, the production rate is assumed to be

$\dot{m}_{pr} = 100 \text{ kg/s}$ . Based on the production rate, the temperature drop is estimated based on the following equations. First, the theoretical number of fractures  $n_{frac}$  in the reservoir is calculated according to Gringarten et al. [14]:

$$n_{frac} = \sqrt{\frac{x_{res} c_{p,water} \dot{m}_{pr}}{2 x_{ED} \kappa_{rock} y_{res} z_{res}}} \quad (6)$$

In this equation,  $x_{res}, y_{res}$  and  $z_{res}$  are the dimensions of the reservoir being 1 km each.  $c_{p,water}$  represents the heat capacity of water at 4.182 kJ/kgK [3] and  $\kappa_{rock}$  the thermal conductivity of rock at 2.5 W/mK [12]. In agreement with other studies and real plant data, the production rate  $\dot{m}_{pr}$  is assumed to be 100 kg/s [33,34]. The variable  $x_{ED}$  represents the dimensionless fracture distance as defined by Doe et al. [15]. In this study, a conservative value of 8 is chosen to ensure thermal independence of the  $n_{frac}$  different fractures [15]. Based on the number of fractures, the dimensionless time  $t_D$  until decommissioning of the geothermal plant after  $t_{lifetime} = 30a$  [35] can be calculated by the following equation derived from Doe et al. [14].

$$t_D = \frac{c_{p,water}^2}{\kappa_{rock} \rho_{rock} c_{p,rock}} \left( \frac{\dot{m}_{pr}}{n_{frac} y_{res} z_{res}} \right)^2 t_{lifetime} \quad (7)$$

Based on this equation, the dimensionless temperature  $T_D$  at the end of the plant lifetime can be calculated using the solution of Gringarten et al. [14]:

$$T_D = f_{Gringarten}(t_D, x_{ED}) \quad (8)$$

The dimensionless temperature  $T_D$  can be formulated directly to the absolute temperature  $T_{pr}$  based on the initial rock temperature  $T_{rock}$  from Section 2.3 and the common injection temperature  $T_{inj}$  of 80 °C [2]:

$$T_{pr} = T_{rock} - T_D (T_{rock} - T_{inj}) \quad (9)$$

Finally, the heat flow at temperature  $T_{pr}$  can be calculated by:

$$\dot{Q}_{pr} = \dot{m}_{pr} \rho_{water} c_{p,water} (T_{pr} - T_{inj}) \quad (10)$$

#### 2.4.4. Power plant modeling

After describing the reservoir models and operating behavior for all three different approaches for reservoir modeling, the conversion of heat into net electrical power is described. For the thermal conversion, the efficiency of existing geothermal plants is approximated [2]:

$$\eta_{plant} := \frac{0.00052}{c} T_{pr} + 0.032 \quad (11)$$

Since the plant requires a minimum temperature to operate, only reservoirs with a host rock temperature of 150 °C [35] are considered. The gross electrical power can be obtained directly from:

$$P_{el,gross} = \eta_{plant} \dot{Q}_{pr}$$

For the circulation of the production water flow, auxiliary electrical power  $P_{aux}$  is used for the pumps. This is modeled based on the pressure difference  $p_{res}$  of the reservoir, which is assumed to be  $\Delta p_{res} = 0.5 \frac{\text{bar}}{\text{kg}} \dot{m}_{pr}$  [36] and the pump efficiency of  $\eta_{pump} = 0.675$  [36].

$$P_{aux} = \frac{\dot{m}_{pr} \Delta p_{res}}{\eta_{pump} \rho_{water}} \quad (12)$$

The average electrical power output of the plant  $P_{el,net}$  over its lifetime is:

$$P_{el,net} = P_{el,gross} - P_{el,aux} \quad (13)$$

#### 2.5. Economic modeling

In addition to the technical modeling, a cost model is required to calculate the average levelized cost of electricity (LCOE) per plant. This involves calculating the levelized cost of electricity over the lifetime of a plant. The investment cost for a plant in 2050 is derived using the following equation and assumptions from Table 2.

$$C_{Inv} = 2 C_{borehole} + C_{plant} + C_{stimulation} + C_{pump} + C_{exploration} \quad (14)$$

The size of the plant  $P_{plant}$  and the pump  $P_{pump}$  are derived from the respective power consumption  $P_{el,gross}$  and  $P_{aux}$  and the average availability factor of a geothermal plant of 0.9 [37]. The interest rate is assumed to be 8 %, the fixed operating costs are assumed to be 2 % of the investment costs per year [12] and the lifetime is assumed to be 30 years [2]. Based on the economical model, the depth with the lowest LCOE is chosen as the reservoir depth up to a maximum technical depth of 7000 m [8].

During the operation of the reservoir, the temperature decreases due to the extraction of thermal heat. Therefore, the reservoir cannot be used indefinitely and is not renewable. To account for the non-renewability of geothermal heat, two variables are introduced. First, the lifetime of the reservoir  $t_{res,lifetime}$ , which measures the time until the reservoir can still be operated, meaning until the minimal technical host rock temperature of 150 °C is reached. Second, the time to thermal regeneration  $t_{reg}$  is defined as the time until the reservoir reaches the initial temperature again through the geological heat flow.

### 3. Results

This study presents the first detailed land eligibility analysis for EGS plants on a global scale to show where geothermal plants can be built and where land restrictions arise (first research question). Then, the different approaches for reservoir simulation are compared to find the most realistic approach (second research question). Finally, the global capacity potential for EGS power generation is shown and the impact on national electricity supply is evaluated (third research question).

#### 3.1. Land eligibility

On a global average, 27.4 % of the Earth's land surface is suitable for the construction of geothermal plants based on the surface land criteria defined in Table 1. Global land eligibility varies from <5 % in North Africa to 72 % in the Central African Republic (see Fig 3). The highest global land eligibilities are found in the boreal forests of the Northern Hemisphere, the steppe of Central Asia, and the savannas of Africa and South America. Land areas for geothermal power of less than 10 % are found in Europe, West Asia and North Africa.

The main reason for non-useable land areas is primarily groundwater scarcity: ~32 % of the global land area cannot be used because the local groundwater resources are not considered sufficient for the water supply of the plant. The areas excluded due to high water scarcity are shown in Fig. 4. The second most relevant exclusion criterion is slope, with ~18 % of the excluded land area mainly in the world's major mountain ranges (see Fig. 4). Nature protection limits ~16 % of the land area from building geothermal plants especially in Central Africa and the Amazon region (see Fig. 4). Cities and villages each prevent 11 % of the world's land from being used for geothermal energy. In densely populated areas such as Europe, settlements are the most relevant criteria (see Fig. 4).

**Table 2**  
Investment cost assumptions of an enhanced geothermal power plant in 2050.

Cost	Values	Source
Borehole	1167E3 € + 258 €/m t + 0.167 €/m <sup>2</sup> t <sup>2</sup>	[36,38]
Plant	1560 €/kW $P_{plant}$	[39]
Stimulation	2.5 M€	[36,40]
Pump	1720 €/kW $P_{pump}$	[39]
Exploration	1.85 M€	[40,41]



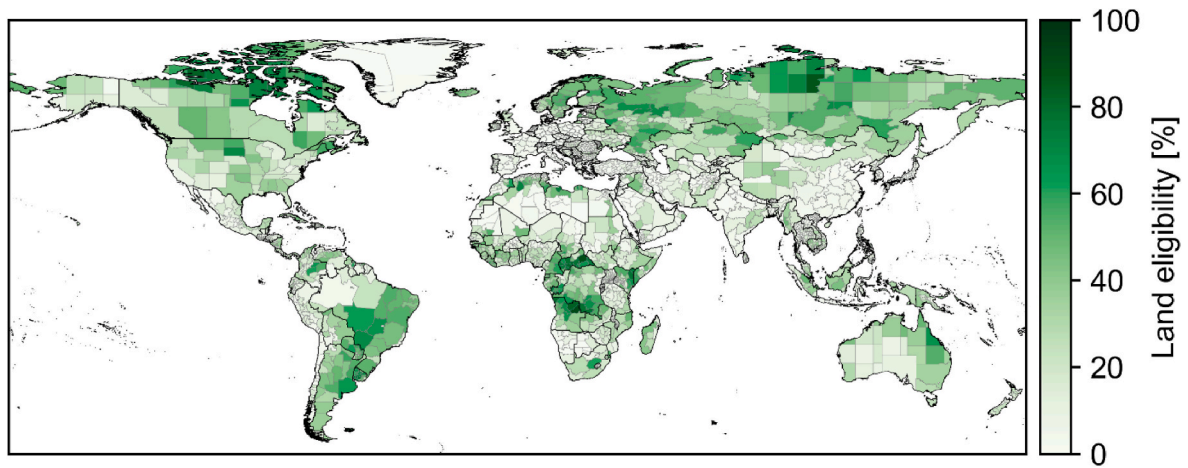


Fig. 3. Global land eligibility for deep geothermal energy.

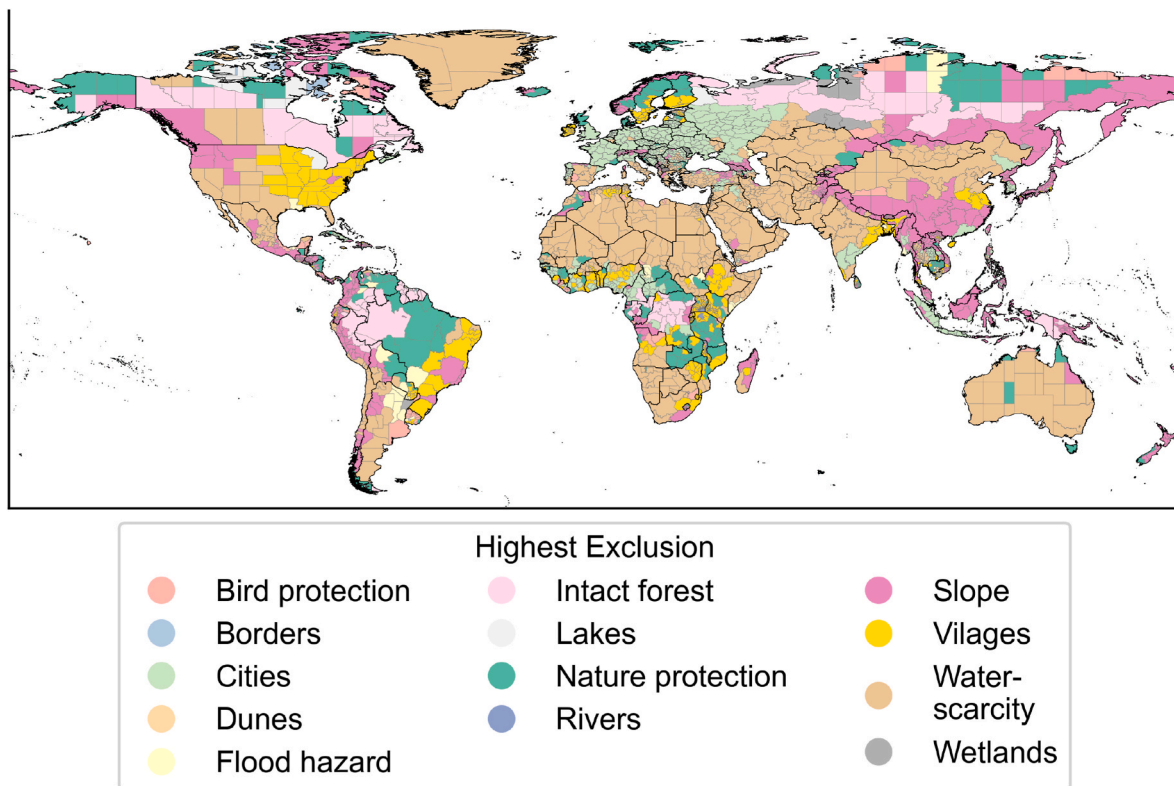


Fig. 4. Criteria with highest land exclusion per region for enhanced geothermal power.

### 3.2. Operation strategy

Within this study, three different operational strategies are evaluated: The Gringarten Method, the Sustainable Approach and the Volume Method. These three different approaches are evaluated to find the most suitable approach for global energy potential in terms of capacity, cost and renewability. The comparison is shown in Fig. 5 as a distribution of plant-specific variables over the set of all global plants derived during the land eligibility analysis.

To highlight the difference in the plant size, the production rate  $\dot{m}_{pr}$  is shown in Fig. 5 for each simulation approach. The plants, when designed according to the Gringarten approach, have a fixed production rate of 100 kg/s. For plants based on the volume method, the production rate is implicitly given based on the temperature drop  $\Delta T$ , the reservoir volume

$V_{res}$  and the recovery factor  $R_F$  and results in production rates of about 10 kg/s. Compared to the volume method, the sustainable volume method assumes no temperature drop and uses only the natural heat flow, which is orders of magnitude lower than the heat stored in the host rock enthalpy  $H_{res,use}$ . Therefore, the production rate is also lower at about 0.1 g/s. This leads directly to different plant sizes, and power outputs. While plants designed based on Gringarten assumptions are at about 1 GW, plants based on the volume method are lower at about 300 MW and the plants from the sustainable volume method at 10 MW. Since the cost of geothermal plants is dominated by their fixed drilling costs, the levelized cost of electricity is highly dependent on the capacity and thus the annual energy produced. Therefore, the plants designed based on the Gringarten approach generate the cheapest electricity at 0.03–0.35 EUR/kWh<sub>el</sub>, followed by the volume method at 0.3–1 EUR/

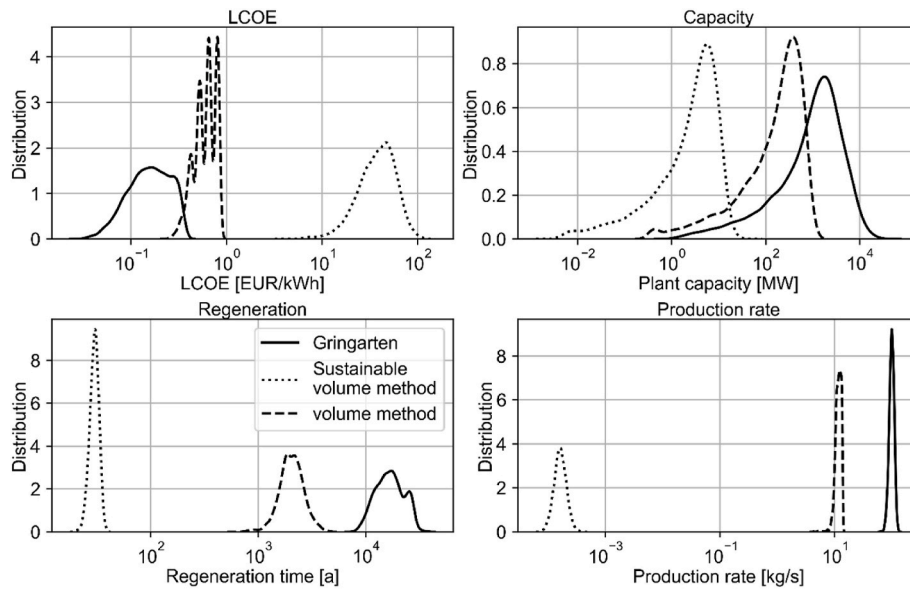


Fig. 5. Comparison of different operation strategy and geothermal models based on different literature approaches.

kWh<sub>el</sub> and the sustainable approach at 10–100 EUR/kWh<sub>el</sub>.

This shows that only the plants based on the Gringarten approach are the only ones which are possibly economically viable. This finding is also consistent with the results for the production rate: While a production rate of 100 kg/s as in the Gringarten model are plausible results used in the economic models of Limberger et al. and Aghahosseini et al. [11,12] and used in actual geothermal plants [34], the production rates resulting from assumptions of the volume method and the sustainable approach are too small and therefore unrealistic. Therefore, only the results from the Gringarten approach led to realistic results. On the other hand, the operation based on Gringarten leads to a much higher average temperature drop over the reservoir: While Gringarten plants reduce the average temperature of the reservoir by 10–30K over the lifetime of 30 years, the results based on the volume method reduce the average reservoir temperature by 1.4K ( $= R_F \Delta T$ ). This results in a large difference in the reservoir regeneration times, which is the time until the natural heat flow could heat up the host rock to the temperature before operation of the plant (see Fig. 5): While plants based on the volume method require 2000 years before the reservoir can be used again after the initial plant lifetime of 30 years, the regeneration time for the Gringarten method is about 20,000 years. Therefore, both strategies are not renewable compared to the time periods in which humanity uses

energy. Instead, if deep geothermal heat is to be harvested, its operation will be exploitative and there will be a limited range to it as further discussed later on. Since the Gringarten approach is the only economically viable and realistic approach, global energy and potential is calculated based on the Gringarten model.

### 3.3. Global capacity potentials

The global technical potential for electricity generation is 12 TW of capacity or 102 PWh/a of electrical energy, which is about 88 % of the global final energy consumption in 2019 [42]. The global distribution is shown in Fig. 6. Large parts of the world are not suitable for geothermal power generation, either because of land eligibility restrictions or because of insufficient geothermal heat below 150 °C. These areas are located in the northern parts of Canada and Russia, Eastern Europe and West Africa. Countries with high capacity potential are distributed across North America (1.17 TW), Brazil and southern parts of South America with 1.1 TW each, Africa (3.6 TW), China (1.0 TW), Australia (1.1 TW), and Southeast Asia (1.4 TW).

The average levelized cost of electricity for each region is shown in Fig. 7. High temperatures lead to a high potential and to low cost. Therefore, the lowest costs are in the same regions as described in Fig. 6:

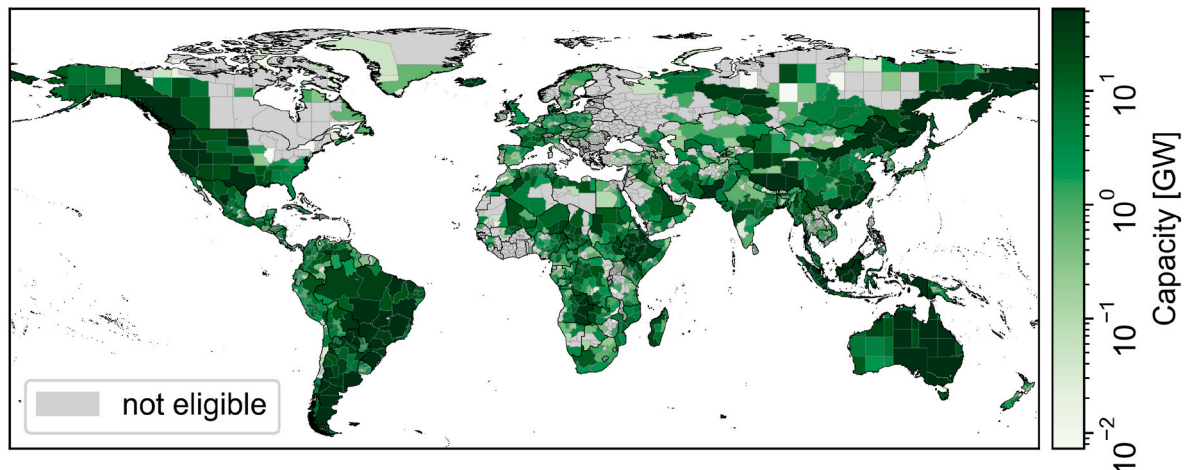


Fig. 6. Global capacity potentials for deep geothermal power plants.

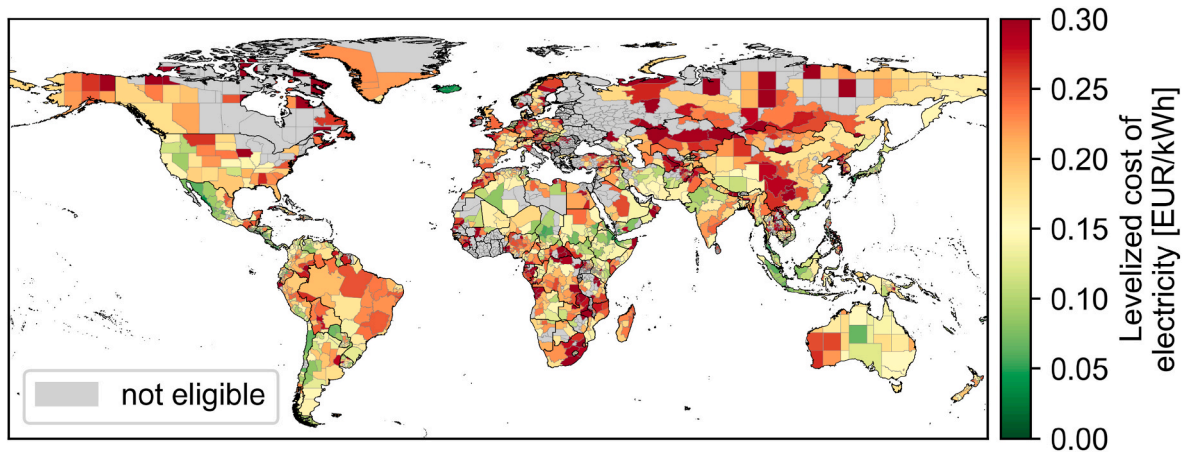


Fig. 7. LCOE for enhanced geothermal power generation based on cost assumptions for the cost year 2050.

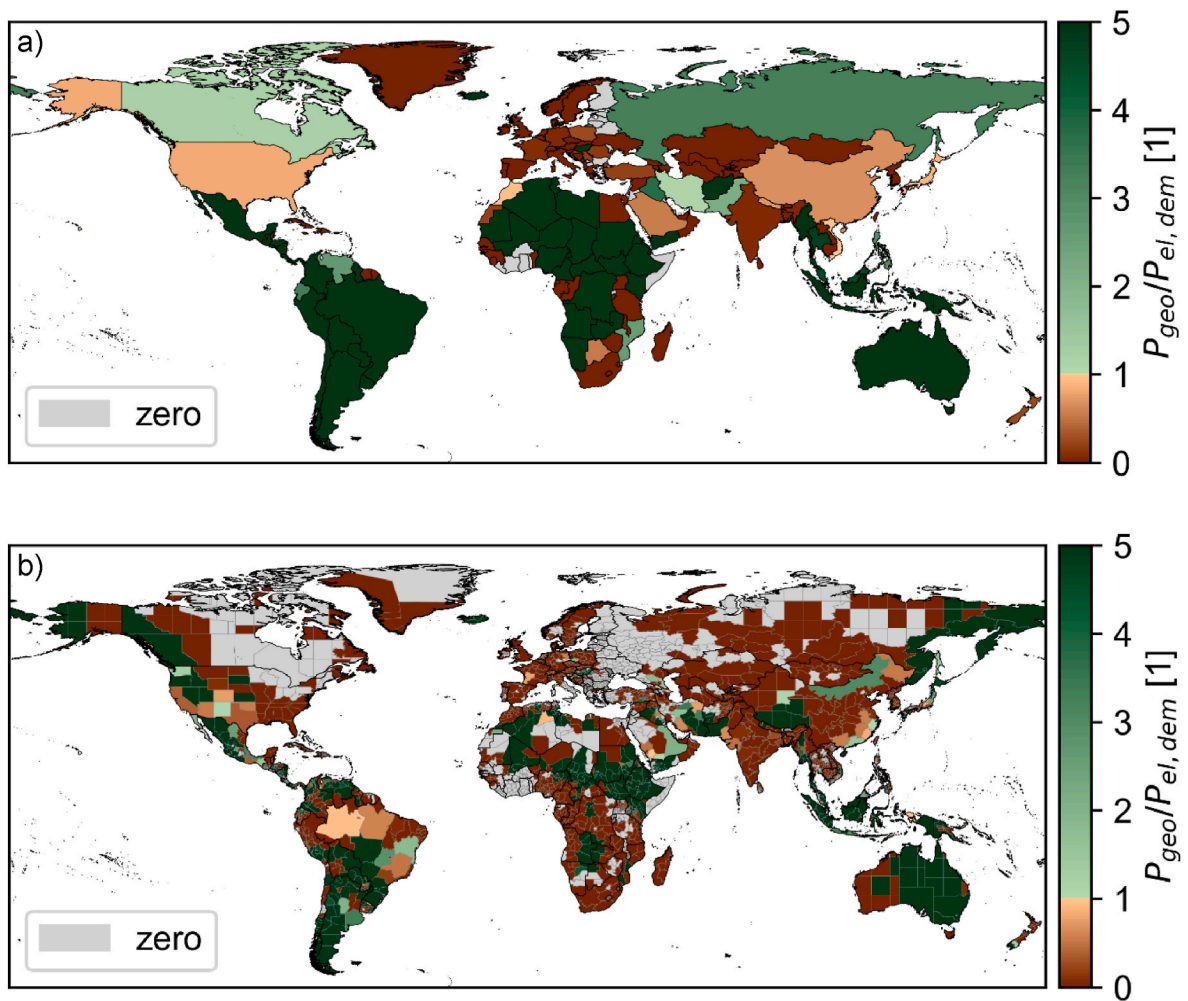


Fig. 8. Capacity potential per 2019 electricity demand of deep geothermal power within a cost range of 0–0.1 EUR/kWh in the cost year 2050 for a) each country and b) each federal state.

starting at 0.04 EUR/kWh in Iceland, East Africa, West Africa, Southern Japan and Southeast Asia. Medium-cost electricity from EGS at up to 0.1 EUR/kWh can be found in South and North America, Africa, Southeast Asia, East Asia and Australia.

#### 3.4. Impact of deep geothermal power on nations power supply

The previous section has shown how large the technical potential of enhanced geothermal power is. Not all of this potential can be economically exploited, as the LCOE is above the current economic cost of geothermal energy at 0.1 EUR/kWh EUR/kWh [37]. To conclude,



Fig. 8 shows the regions of the world where deep geothermal energy can play a role in the future, where the energy potential is below the threshold of 0.1 EUR/kWh.

The figure shows the ratio  $P_{geo}/P_{dem,el}$  to indicate the ratio of a country's economic energy potential from EGS to its electricity demand [43]. This map highlights those regions of the world where deep geothermal energy may play a role in the future. Regions with a high and cheap energy potential for deep geothermal power generation are located in Central and South America including Mexico, Africa and Southeast Asia. Most countries in these regions can supply more than five times their electricity demand from geothermal power on a national level. African countries, in particular, have a high relative energy potential of more than 100 times their electricity demand and up to 7000 times in Tchad due to their currently low electricity demand. Other economic energy potential is more widely distributed around the world: Both Canada and Russia could meet all their electricity demand with deep geothermal power plants at costs below 0.1 EUR/kWh. In both countries, however, the spatial overlap of EGS-potential and demand centers is only limited to part of the countries. In Canada, only Vancouver can profit from EGS-potential, whereas deep geothermal energy from north-west might be unused. While Russia theoretically could harvest enough energy on a national scale, the technical EGS potential can be found in east Russia, far away from the demand centers in west Russia. In Europe, low-cost geothermal potential can only be found in Iceland and Hungary, both of which can supply 25 and 6 times their countries electricity demand, respectively. Other countries with high economic potential include Myanmar, Thailand and Afghanistan. Some developed countries also have high low-cost potential: Japan could meet 92 % of its annual electricity demand from deep geothermal power. This is followed by China (68 %), the US (83 %) and Poland with 27 %. Germany could meet only 7 % of its electricity demand from deep geothermal power in 2019 at less than 0.1 EUR/kWh.

The lowest cost energy potential of EGS below 0.05 EUR/kWh is found in only 17 countries. Their potential-cost curve is shown in Fig. 9. The absolute lowest costs at 0.03 EUR/kWh are found in Mexico, Russia and Japan directly followed by Iceland, Thailand and China below 0.035 EUR/kWh. Since the capacity of a plant is inversely proportional to the LCOE (see Supplementary Data), most low-cost countries can meet their entire electricity demand from geothermal power at costs below 0.06 EUR/kWh. The only exceptions are Japan, with its small land surface area, and China, with its huge electricity demand. The most promising candidates for nationwide large-scale deep geothermal power generation are Iceland with >5 times its electricity demand below 0.04 EUR/kWh, Thailand with 3.5 times its electricity demand at 0.04 EUR/kWh

and Mexico with once its electricity demand at 0.04 EUR/kWh.

#### 4. Discussion

From the three different considered simulation approaches, only the Gringarten approach is economically viable: The technical capacity potential based on the volume method and the sustainable method resulted in unrealistically small mass flows and therefore high costs. Due to the decrease of enthalpy of the reservoir, enhanced geothermal power, if economically viable, is not renewable with regeneration times greater than 20,000 years based on the natural heat flow after 30 years of use. The realization that geothermal energy is not renewable at a given location for a given reservoir has major implications for its use within energy systems. For example, Japan could approximately supply roughly its own annual demand by geothermal energy for 30 years once, which means that Japan would first exploit its reservoirs at the optimal depth (usually 7000 m). This depletion could be repeated at non-cost-optimal shallower depths resulting in an increase in cost of 6–12 % at the next depth layer. However, the depletion of non-renewable reservoirs needs to be further considered in energy system transformation pathways.

This study showed, that 17 countries can produce geothermal energy at costs below 0.05 €/kWh in 2050 and that energy potentials below 0.1 €/kWh in 2050 are mostly found in developing countries [44] in the Americas, Africa and Southeast Asia. Compared to the electricity costs of onshore wind at 0.02–0.03 €/kWh [45] and PV below 0.02 €/kWh [46], enhanced geothermal power will be more expensive, but can still offer better dispatchability due to its higher capacity factor of up to 0.9 compared to wind at 0.37 [45]. Due to the non-trivial pricing of stability within energy systems, the break-even point for cost vs. dispatchability is still uncertain. Therefore, no threshold for the economic potential can be established for this study. Nevertheless, for the 17 hot-spot countries, enhanced geothermal power is a great opportunity to be used as a dispatchable energy source to stabilize the energy. For most of the developing world in Africa, the Americas and Southeast Asia, geothermal power can play an important role in stable renewable energy systems. The future cost development of geothermal power is largely dependent on the future drilling costs, which are assumed to be reduced to ~33 % of current costs at 7000m in the US Department of Energy's future drilling cost estimation [38]. Therefore, the potential use in developing countries is highly dependent on technology development. Developed countries also have a large capacity potential of geothermal power in the USA, Japan, China, Iceland and Hungary, but due to their large energy demands, they can only partially use geothermal heat for their energy

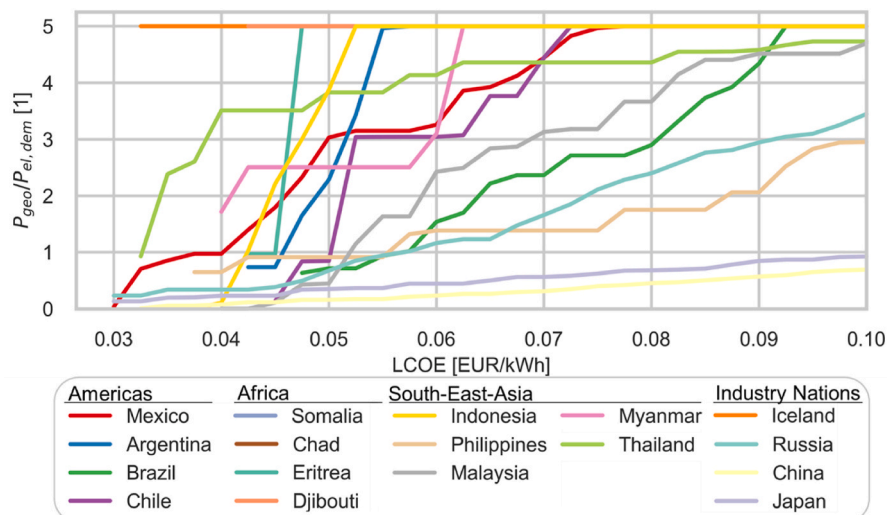


Fig. 9. Capacity potential per 2019 electricity demand of deep geothermal power for all countries with lowest LCOE below 0.05 EUR/kWh for the cost year 2050.



demands at costs below 0.1 €/kWh. Nevertheless, enhanced geothermal energy can be a promising option for future power generation in these countries as well.

Compared to the results of other studies on enhanced geothermal power, this study is within the literature range. For example, in Europe, literature capacities (at a given depth per site) range from 441 GW<sub>el</sub> to 1711 GW<sub>el</sub> [10], while this study shows 500 GW<sub>el</sub>. For the USA, the literature estimates a capacity potential of 1678 GW<sub>el</sub> [9] to 7272 GW<sub>el</sub> [12], while this study shows 1188 GW<sub>el</sub>. Interestingly, this is only by chance as there are two counterbalancing deviations found. First, this paper is the only one that considers a detailed land eligibility analysis, with only two publications in the literature considering land eligibility constraints at all. Also, this publication is the only one that considers the exchange of adjacent reservoirs, which further reduces the energy potential by a factor of 4. Therefore, this publication has a reduced horizontal area by an order of magnitude, which can be explained by a more detailed catalog of assumptions. On the other hand, this publication assumes a much higher temperature drop of the reservoir to account for a much more realistic production rate, which is an order of magnitude higher than the production rate implicitly included in the technical models of other studies (see Fig. 5). Therefore, the effects of different land eligibility approaches and reservoir simulation or operation approaches cancel each other out. Further details on the comparison can be found in the supplementary data. It should be noted that all capacities are calculated and therefore compared for the use of a cost-optimal depth at the same time for a given plant. For example, Tester et al. [2] calculate the power potential for all heat layers at once, which would double the electrical capacity for the maximum depth of 7000m. However, this work considers the optimal depth at a time to account for the techno-economic optimal design of the specific plant.

This study presents a site-specific approach for the land eligibility analysis of geothermal energy. However, it is important to acknowledge the inherent uncertainties in this method. The resolution of geological temperatures is limited to  $0.5^\circ \times 0.5^\circ$  due to constraints of data on geological temperatures and properties as pointed out in section 2.3. Localized geological anomalies and sub-grid heterogeneity are not represented with this approach, as rock properties are only described at this resolution. Results derived from this approach should therefore be interpreted within the limits of the grid-level discretization, and conclusions below this resolution are not possible. To address this limitation, the analysis in this work was conducted at the federal state level, ensuring consistency with the resolution of the input data. The location-specific calculation and processing of data is still beneficial to evaluate the land eligibility analysis and expand the current understanding of technical potentials for enhanced geothermal systems.

Within this study, we apply a widely used methodology for modeling the cost of enhanced geothermal systems, consistent with previous studies in this field. This approach assumes that drilling costs depend only on depth for a given diameter and casing type, while all other specific costs remain constant (see Table 2). This methodology allows for a globally consistent cost comparison for EGS plants. However, the cost model commonly used in this field does not account for global variations in geological conditions, investment costs and interest rates. While geological conditions in general can significantly impact drilling time, complexity and therefore costs, their impact is simplified in global studies for two reasons: First, deep geothermal wells typically extend into the crystalline basement, where geological conditions are more uniform compared to shallower formations. Second, while the structure of the sedimentary cover may vary, large-scale technical potential studies aim for average results over large areas, which mitigates local geological effects. While site-specific geological conditions introduce cost variations for local projects, global studies cannot and do not need to account for regionalized effects due to averaging effects. In a global study, regional economic differences in projects can have an impact on

costs. Currently, there is limited data on the variation in investment conditions for renewable energy worldwide. The International Energy Agency [47] has taken a first step by considering different capital investments for four regions, but only for PV and wind power. Given the much smaller scale of EGS deployment compared to wind power and PV, data on global investment costs are even scarcer. Given these limitations, this study follows the established approach of assuming constant investment costs to ensure comparability, while acknowledging that economic and geological variability may lead to deviations in real-world project costs.

## 5. Conclusion

Based on the analysis and discussion, four main conclusions can be drawn from this work:

This is the first work to conduct a detailed global land eligibility analysis. The land eligibility for enhanced geothermal systems varies significantly depending on local conditions, ranging from <5 % to 72 %, with a global average of 25 %. Key factors influencing eligibility include groundwater, slope, nature conservation, settlements, intact forests, and water bodies. Therefore, a detailed land eligibility analysis is crucial for determining the global technical potential for deep geothermal energy.

This work is the first to directly link the technological model with the economic model of enhanced geothermal plants in the field of technical potential analysis. This approach shows that currently used models assuming a thermal drawdown of 10 K for a lifetime of 30 a can only achieve leveled costs of electricity above 30 ct<sub>EUR</sub>/kWh, which is not economic. An economically feasible operation of an EGS plant can be modeled using Gringarten's approach with a production rate of 100 kg/s, resulting in a thermal drawdown of the reservoir of 10–30 K.

To recover the thermal drawdown of the reservoir by means of the natural heat flow in the economic scenario would take more than 20,000 years. Therefore, deep geothermal power is not renewable within a reasonable usage period of use by mankind.

High-potential, low-cost geothermal energy is concentrated in certain regions. Seventeen countries could generate power below 0.05 €/kWh by 2050, with the highest potential being in Iceland, the US, China, Japan, Hungary, and Russia. However, EGS remains more expensive than wind and solar but offers a better dispatchability.

## CRedit authorship contribution statement

**D. Franzmann:** Writing – review & editing, Writing – original draft, Validation, Software, Methodology, Investigation, Formal analysis, Data curation, Conceptualization. **H. Heinrichs:** Writing – review & editing, Writing – original draft, Supervision, Resources, Funding acquisition. **D. Stolten:** Writing – review & editing, Supervision.

## Declaration of competing interest

The authors declare that they have no known competing financial interests or personal relationships that could have appeared to influence the work reported in this paper.

## Acknowledgements

This work was supported by the Helmholtz Association under the program "Energy System Design". Additionally, this work was partly funded by the European Union (ERC, MATERIALIZE, 101076649). Views and opinions expressed are, however, those of the authors only and do not necessarily reflect those of European Union.

We would also like to thank Rachel Maier and Maximilian Stargardt for the discussion of the results and their implications.

## Appendix

**Table 3**  
Detailed criteria and datasets used for the land eligibility analysis

Category	Buffer distance [m]	Data source
Urban Settlements	2000	[48,49]
Isolated Building	300	[48,49]
Airport	2000	[50]
Airfield	300	[50]
Primary streets	100	[50]
Secondary streets	100	[50]
Railways	100	[50]
Cable cars	100	[50]
Power lines	100	[50]
Pipelines	100	[50]
Slope (17°)	100	[51]
Borders	500	[52]
Military areas	100	[50]
Nature protection	300	[53]
Bird protection areas	300	[54]
Intact forests	300	[19,55]
Dunes	900	[50]
Industrial areas	300	[50]
Commercial areas	300	[50]
Mines	2000	[50,56]
Coasts	0	[52]
Flood areas	0	[57]
Lakes, Rivers, Creeks	0	[58,59]
Wetlands	0	[49]
Recreation, camping, historical landmarks	300	[50]

## Data availability

Global Technical Energy Potentials of Enhanced Geothermal Systems  
(Original data) (Mendeley Data)

## References

- [1] B. van der Zwaan, Longa F. Dalla, Integrated assessment projections for global geothermal energy use, *Geothermics* 82 (2019) 203–211.
- [2] J.W. Tester, The Future of Geothermal Energy: Impact of Enhanced Geothermal Systems (EGS) on the United States in the 21st Century (2006).
- [3] I. Stober, K. Bucher, in: *Geothermal Energy: from Theoretical Models to Exploration and Development*, second ed., Springer International Publishing; Imprint Springer, Cham, 2021.
- [4] Office of ENERGY EFFICIENCY & RENEWABLE ENERGY, Enhanced geothermal systems, Available from: <https://www.energy.gov/eere/geothermal/enhanced-geothermal-systems>, September 11, 2024.
- [5] A. Pollack, R. Horne, T. Mukerji, What Are the Challenges in Developing Enhanced Geothermal Systems (EGS)? Observations from 64 EGS Sites, 2020.
- [6] Nasa, Technology Readiness Levels (2023).
- [7] G.R. Beardsmore, L. Rybach, D.D. Blackwell, C. Baron, A Protocol for Estimating and Mapping Global EGS Potential, Unpublished, 2011.
- [8] R. Jung, S. Röhling, N. Ochmann, S. Rogge, R. Schellschmidt, Abschätzung des technischen Potenzials der geothermischen Stromerzeugung und der geothermischen, Kraft-Wärmekopplung (KWK) in, Deutschland, 2002.
- [9] C. Augustine, A Methodology for Calculating EGS Electricity Generation Potential Based on the Gringarten Model for Heat Extraction From Fractured Rock, 2017.
- [10] C.R. Chamorro, J.L. García-Cuesta, M.E. Mondéjar, A. Pérez-Madrado, Enhanced geothermal systems in Europe: an estimation and comparison of the technical and sustainable potentials, *Energy* 65 (2014) 250–263.
- [11] J. Limberger, P. Calcagno, A. Manzella, E. Trumpy, T. Boxem, M.P.D. Pluymaekers, et al., Assessing the prospective resource base for enhanced geothermal systems in Europe, *Geoth. Energ. Sci.* 2 (1) (2014) 55–71.
- [12] A. Aghahosseini, C. Breyer, From hot rock to useful energy: a global estimate of enhanced geothermal systems potential, *Appl. Energy* 279 (2020) 115769.
- [13] D. Ryberg, M. Robinius, D. Stolten, Evaluating land eligibility constraints of renewable energy sources in Europe, *Energies* 11 (5) (2018) 1246.
- [14] A.C. Gringarten, J.P. Sauty, A theoretical study of heat extraction from aquifers with uniform regional flow (1975).
- [15] T. Doe, R. McLaren, W. Dershowitz, Discrete fracture network simulations of enhanced geothermal systems, *PROCEEDINGS, Thirty-Ninth Workshop on Geothermal Reservoir Engineering* (2014).
- [16] D.S. Ryberg, GLAES framework: Jülich Systems Analysis ICE2 (2022).
- [17] G.H. Garrison, S.p. Guðlaugsson, L. Ádám, A. Ingimundarson, T.T. Cladouhos, S. Petty, The south Hungary enhanced geothermal System(SHEGS) demonstration project, *GRC Transactions* 40 (2016).
- [18] Y. Peng, H. Azadi, L. Yang, J. Scheffran, P. Jiang, Assessing the siting potential of low-carbon energy power plants in the yangtze river Delta: a GIS-based approach, *Energies* 15 (6) (2022) 2167.
- [19] Intact Forest Landscape. Intact forest landscape; Available from: [www.intactforests.org](http://www.intactforests.org).
- [20] R. Hofste, S. Kuzma, S. Walker, E. Sutanudjaja, M. Bierkens, M. Kuijper, et al., Aqueduct 3.0: updated decision-relevant global water risk indicators, *WRIPUB* (2019).
- [21] S.K. Sanyal, S.J. Butler, in: *An Analysis of Power Generation Prospects from Enhanced Geothermal Systems*, 2005.
- [22] M.L. McLean, D.N. Espinoza, Thermal distressing: implications for short-circuiting in enhanced geothermal systems, *Renew. Energy* 202 (2023) 736–755.
- [23] C.J. Willems, H.M. Nick, G.J. Weltje, D.F. Bruhn, An evaluation of interferences in heat production from low enthalpy geothermal doublets systems, *Energy* 135 (2017) 500–512.
- [24] G. Laske, G. Maske, A Global Digital Map of Sediment Thickness (1997).
- [25] S. Huang, H.N. Pollack, P.Y. Shen, Temperature trends over the past five centuries reconstructed from borehole temperatures, *Nature* 403 (6771) (2000) 756–758.
- [26] I.M. Artemieva, Global 1°×1° thermal model TC1 for the Continental lithosphere: implications for lithosphere secular evolution, *Tectonophysics* 416 (1–4) (2006) 245–277.
- [27] A. Aghahosseini, C. Breyer, Assessment of geological resource potential for compressed air energy storage in global electricity supply, *Energy Convers. Manag.* 169 (2018) 161–173.
- [28] J. Hartmann, N. Moosdorf, The new global lithological map database GLiM: a representation of rock properties at the Earth surface, *G-cubed* 13 (12) (2012).
- [29] B. Goutorbe, J. Poort, F. Lucazeau, S. Raillard, Global heat flow trends resolved from multiple geological and geophysical proxies, *Geophys. J. Int.* 187 (3) (2011) 1405–1419.
- [30] NASA Langley Research Center (LaRC), POWER Project, 2021.
- [31] T. Tischner, B. Melchert, A. Ortiz, M. Schindler, J. Scheiber, A. Genter, Test- Und Probetrieb Des HDR-Kraftwerks Soultz, Abschlussbericht, 2013.
- [32] J.H. Schön (Ed.), *Physical Properties of Rocks: Fundamentals and Principles of Petrophysics*, Elsevier, Amsterdam, New York, 2015.
- [33] J. Limberger, T. Boxem, M. Pluymaekers, D. Bruhn, A. Manzella, P. Calcagno, et al., Geothermal energy in deep aquifers: a global assessment of the resource base for direct heat utilization, *Renew. Sustain. Energy Rev.* 82 (2018) 961–975.
- [34] re3data.org, Geothermal Information System: re3data.org - Registry of Research Data Repositories (2013).
- [35] J.W. Tester, B.J. Anderson, A.S. Batchelor, D.D. Blackwell, R. DiPippo, E.M. Drake, et al., Impact of enhanced geothermal systems on US energy supply in the twenty-first century, *Philos. Trans. A Math. Phys. Eng. Sci.* 365 (1853) (2007) 1057–1094.
- [36] G. Mines, GETEM User Manual (2016).

- [37] International Renewable Energy Agency, Renewable Power Generation Costs in 2022 (2023). Abu Dhabi.
- [38] U.S. Department of Energy, GeoVision: Harnessing the Heat Beneath Our Feet (2019).
- [39] P. Heidinger, J. Dornstädter, A. Fabritius, HDR economic modelling: The HDRec Software (2006).
- [40] K.F. Beckers, M.Z. Lukawski, B.J. Anderson, M.C. Moore, J.W. Tester, Levelized costs of electricity and direct-use heat from enhanced geothermal systems, *J. Renew. Sustain. Energy* 6 (1) (2014) 13141.
- [41] G. Mines, J. Nathwani, Estimated Power Generation Costs for EGS, Thirty-Eighth Workshop on Geothermal Reservoir Engineering, 2013.
- [42] International Energy Agency, Key World Energy Statistics 2021: Final consumption (2021).
- [43] Statistics Division United Nations. Energy balance visualization; Available from: <https://unstats.un.org/unsd/energystats/dataPortal/>.
- [44] UNCTAD. UNCTADstat (2023).
- [45] International Renewable Energy Agency, Future of wind: deployment, investment, technology, grid integration and socio-economic aspects, Abu Dhabi: International Renewable Energy Agency (2019).
- [46] D. Franzmann, H. Heinrichs, F. Lippkau, T. Addanki, C. Winkler, P. Buchenberg, et al., Green hydrogen cost-potentials for global trade, *Int. J. Hydrogen Energy* (2023).
- [47] IEA, World Energy Outlook 2023 (2023).
- [48] European Commission, Joint Research Centre. GHSL Data Package 2023, Publications Office, 2023.
- [49] Marcel Buchhorn, Bruno Smets, Luc Bertels, Bert De Roo, Myroslava Lesiv, Nandin-Erdene Tsendbazar, et al., Copernicus Global Land Service: Land Cover 100m: Collection 3: Epoch 2019: Globe, Zenodo, 2020.
- [50] OpenStreetMap contributors, Planet dump, retrieved from, <https://planet.osm.org>, 2020.
- [51] OpenTopography, ALOS World 3D - 30m: OpenTopography (2016).
- [52] GADM. GADM maps and data; Available from: <https://gadm.org/about.html>.
- [53] UNEP-WCMC and IUCN, Protected planet, The World Database on Protected Areas (WDPA) (2021) [December 10, 2021]; Available from: The World Database on Protected Areas (WDPA)/.
- [54] BirdLife International. Digital boundaries of important bird and biodiversity areas from the world database of key biodiversity areas: september 2020 version; Available from: <http://datazone.birdlife.org/site/requestgis>.
- [55] P. Potapov, M.C. Hansen, L. Laestadius, S. Turubanova, A. Yaroshenko, C. Thies, et al., The last frontiers of wilderness: tracking loss of intact forest landscapes from 2000 to 2013, *Sci. Adv.* 3 (1) (2017) e1600821.
- [56] V. Maus, S. Giljum, J. Gutschlhofer, D.M. Da Silva, M. Probst, S.L.B. Gass, et al., Global-Scale Mining Polygons, PANGAEA, 2020 (Version 1).
- [57] Dottori F, Alfieri L, Salamon P, Bianchi A, Feyen L, Hirpa F. Flood hazard map of the world - 20-Year return period; Available from: [http://data.europa.eu/89h/jrc-floods-floodmapgl\\_rp20y-tif](http://data.europa.eu/89h/jrc-floods-floodmapgl_rp20y-tif).
- [58] M.L. Messenger, B. Lehner, G. Grill, I. Nedeva, O. Schmitt, Estimating the volume and age of water stored in global Lakes using a geo-statistical approach, *Nat. Commun.* 7 (2016) 13603.
- [59] G.H. Allen, T.M. Pavelsky, Global extent of Rivers and streams, *Science* (New York, N.Y.) 361 (6402) (2018) 585–588.